

β -K₄La₆I₁₄Os: A New Structure Type for Rare-Earth-Metal Cluster Compounds That Contains Discrete Tetrahedral K₄I³⁺ Units

S. Uma and John D. Corbett*

Department of Chemistry, Iowa State University, Ames, Iowa 50011

Received January 12, 1999

Suitable reactions of KI, La, LaI₃, and Os in niobium tubes at 800–850 °C result in black, air- and moisture-sensitive crystals of the quaternary title phase. Isostructural K₄Pr₆I₁₄Z also exist for Z = Fe, Ru. The title phase was characterized by single-crystal X-ray diffraction (tetragonal, *P4/ncc* (No. 130), *Z* = 4; *a* = 13.117(3), *c* = 25.17 (1) Å at 23 °C). The important structural feature is the constitution (K₄I)³⁺(La₆I₁₃Os³⁻) with a new type of 3D anion network of [(La₆Os)I₈I^{-a}_{4/2}I⁻ⁱ_{4/2}I^{a-a}_{2/2}] clusters that are connected into puckered layers through I^{-a} and I⁻ⁱ atom pairs that bridge diagonally in the *a*-*b* plane. These cluster layers are further interlinked along *c* at trans-vertexes through simple bridging I^{a-a}. The 14th iodine atom occurs in the unique K₄I³⁺ ions which lie in columns that interpenetrate the La₆OsI₁₃ network along *c*. The present 16-e⁻ clusters, in contrast with the optimal 18-e⁻ octahedral cluster configuration, exhibit an uncommon tetragonal elongation and evidently become closed shell, with only a small temperature-independent (van Vleck-like) paramagnetism, $\sim 4 \times 10^{-4}$ emu mol⁻¹.

Introduction

The remarkable stabilities of R₆X₁₂-type cluster halides in which a rare-earth-metal (R) octahedron is centered by a transition metal have resulted in many new structure types with different compositions. The bonding systematics within and around R₆X₁₂Z cluster units appear to be well established.^{1,2} The 12 edges of the metal octahedron are always edge-bridged by inner halides Xⁱ, and the exo positions at each metal vertex are also bonded to an outer halide, X^a. The latter may originate from Xⁱ (as bifunctional X^{a-i}) in other clusters, from simple intercluster bridging X^{a-a}, from a solely terminal X^a, or, in rare cases, from X^{a-a-i} or X^{a-a-a} bridging functions. The interstitials provide both central R-Z bonding and additional valence electrons for the R-Z and R-R bonding in these relatively electron-poor clusters.³ Possible interstitial atoms are late transition metals (group 7–11 elements), main-group elements (Be–N, Si, etc.), and even small dimers such as C₂. Structural diversity is often achieved by varying *Z* and also the X:R proportion.

Finally, the introduction of alkali-metal cations within the cavities of the halide network may alter both the structures and the number of cluster-based electrons. Many quaternary examples with a wide range of structural diversity are known among the zirconium halides.^{1,2} The corresponding reduced rare-earth-metal halides include the earlier examples with main-group interstitials, such as Cs₄Pr₆I₁₃C₂, Cs₄Sc₆I₁₃C,⁴ Cs₂Pr₆I₁₂C₂,⁵ and CsEr₆I₁₂C.⁶ Subsequent transition-metal-stabilized discoveries

include Cs₄R₆I₁₃Z (R = Ce, Pr; Z = Co, Os),⁷ AR₆I₁₀Z (A = K, Cs; R = La, Ce, Pr; Z = Mn, Fe, Os),⁸ biclusters in A₂R₁₀I₁₇Z₂ (A = Rb, Cs; R = La, Ce, Pr; Z = Co, Ni, Ru, Os),^{9,10} K₂La₆I₁₂Os,¹¹ and α -K₄La₆I₁₄Os.¹²

Exploratory solid state synthesis seems to be the only workable route to new phases because of a general inability to predict relative phase stabilities and thence structures or compositions. We report here the synthesis of a new compound which is a nominal polymorph of the novel tetragonal (α)-K₄-La₆I₁₄Os,¹² in which undistorted octahedral La₆(Os)I₁₀ units are interbridged by I^{-a}_{4/2}I^{a-i}_{4/2} into a new planar network. The present β -K₄La₆I₁₄Os is instead constituted as (K₄I)³⁺La₆(Os)I₁₃³⁻ with a new high-symmetry anion network for that composition with just the right cavity dimensions for the 14th iodine to be bound to all of the potassium ions as tetrahedral (K₄I)³⁺ ions. Discrete tetrahedral (A₄Br)³⁺ (A = Na–Cs) ions have been seen previously only in the bromine-rich zirconium cluster compounds (A₄Br)₂Zr₆Br₁₈Z (A = Na, K, Rb; Z = some H, Be, B, Mn) and (Cs₄Br)Zr₆Br₁₆B.¹³ Interestingly, the necessary packing in all of these generates well-defined cation sites for these tetrahedra rather than the poorly defined low-symmetry sites that are often present in compounds with simple cations.

Experimental Section

Syntheses. Reactions were carried out in welded Nb or Ta containers¹⁰ utilizing R, RI₃, KI or K, and transition elements Z. The R metals La and Pr (Ames Laboratory, 99.99%), K (Baker, under Ar), and the transition metals Fe, Ru, and Os (Alfa, 99.95%) were used as received. The alkali-metal iodides (Fisher, 99.95%) were dried under

- (1) (a) Corbett, J. D. In *Modern Perspectives in Inorganic Crystal Chemistry*; Parthé, E., Ed.; Kluwer Academic Publishers: Dordrecht, The Netherlands, 1992; p 27. (b) Corbett, J. D. *J. Alloys Compd.* **1995**, *224*, 10.
- (2) Simon, A.; Mattausch, H.; Miller, G. J.; Bauhofer, W.; Kremer, R. K. In *Handbook on the Physics and Chemistry of the Rare Earths*; Gschneider, K. A., Jr., Eyring, L., Eds.; Elsevier Science Publishers B.V.: Amsterdam, 1991; Vol. 15, p 191.
- (3) Hughbanks, T. *Prog. Solid State Chem.* **1989**, *19*, 329.
- (4) Artelt, H. M.; Meyer, G. Z. *Anorg. Allg. Chem.* **1994**, *620*, 1521.
- (5) Artelt, H. M.; Schleid, T.; Meyer, G. Z. *Anorg. Allg. Chem.* **1992**, *618*, 18.

- (6) Artelt, H. M.; Meyer, G. Z. *Anorg. Allg. Chem.* **1993**, *619*, 1.
- (7) Lulei, M.; Corbett, J. D. *Inorg. Chem.* **1996**, *35*, 4084.
- (8) Lulei, M.; Corbett, J. D. *Z. Anorg. Allg. Chem.* **1996**, *622*, 1677.
- (9) Lulei, M.; Maggard, P. A.; Corbett, J. D. *Angew. Chem., Int. Ed. Engl.* **1996**, *35*, 1704.
- (10) Lulei, M.; Martin, J. D.; Hoistad, L. M.; Corbett, J. D. *J. Am. Chem. Soc.* **1997**, *119*, 513.
- (11) Uma, S.; Corbett, J. D. *Inorg. Chem.* **1998**, *37*, 1944.
- (12) Uma, S.; Martin, J. D.; Corbett, J. D. *Inorg. Chem.* **1999**, *38*, 3825.
- (13) Qi, R.-Y.; Corbett, J. D. *Inorg. Chem.* **1997**, *36*, 6039.

dynamic vacuum and then sublimed. All operations were carried out in N₂-filled gloveboxes owing to the air and moisture sensitivity of some of the reagents and all of the products.

The unknown β -K₄La₆I₁₄Os was first obtained in ~90% yield from the precise composition of the previously characterized α -K₄La₆I₁₄Os,¹² as was subsequently established by comparison of the Guinier powder pattern of the former with the one calculated after the structural solution. Synthesis reaction mixtures were all heated between 800 and 850 °C for 27 days and then cooled to 300 °C at 5 °C h⁻¹. The phase was also seen in 70% yield from the loaded compositions K₆La₆I₁₆Os (along with 15% LaOI and a few unidentified lines) and K₈La₆I₁₅Os (together with 15% KI and 10% LaOI), but analogous Fe and Ru derivatives could not be made. However, additional reactions of the compositions K₄Pr₆I₁₄Fe and K₄Pr₆I₁₄Ru resulted in ~40% yields of the corresponding β -K₄Pr₆I₁₄Z along with ~20% KPr₂I₁₀Z,¹⁴ 10% PrOI, and additional lines. The refined lattice constants for K₄Pr₆I₁₄Fe were $a = 13.117(3)$, $c = 25.17(1)$ Å.

Single-Crystal X-ray Studies. Small irregular black crystals of β -K₄La₆I₁₄Os were sealed in thin-walled capillaries in the glovebox, and their singularity was checked by Laue photographs on Weissenberg cameras. Many were multiple. The tetragonal cell parameters and the orientation matrix were obtained from an approximately 0.1 × 0.09 × 0.08 mm crystal via a least-squares refinement of the setting angles of 25 centered reflections located on a Rigaku AFC6R diffractometer operating with graphite-monochromated Mo K α radiation. A total of 10 082 reflections were measured ($4 \leq 2\theta \leq 55^\circ$; $\pm h, \pm k, l$; ω scan) at room temperature. These gave 2950 unique data of which 799 were observed ($I > 3\sigma_I$). The observation of all orders of hkl along with the absences of $hk0$, $h + k \neq 2n$, $0kl$, $l \neq 2n$, was taken as support of the choice of the unique tetragonal space group $P4/ncc$ (No. 130). There were actually four weak violations of this condition ($4 \leq I_0/\sigma_I \leq 7$) that were rejected at the beginning. The correctness of the Laue and space group selections was later proven by the successful refinement.

The structure was solved by direct methods (SHELXS¹⁵). Refinement programs, scattering factors, etc. were those in the TEXSAN package.¹⁶ An empirical absorption correction ($\mu = 190.02 \text{ cm}^{-1}$) was first applied to the full data set with the aid of three ψ scans measured near $\chi = 90^\circ$ [$R_{\text{int}}(I > 5\sigma_I) = 15.5\%$]. The structural model using the heavy atoms identified by the direct methods refined well, and the location of K was obtained with the aid of a difference Fourier map. The difference map also indicated still another but isolated iodine atom that was at a reasonable distance from a tetrahedron of surrounding K atoms and defined the polycation (K₄I)³⁺. The absorption was further corrected after isotropic refinement by DIFABS, as recommended¹⁷ (relative transmission coefficient range: 0.444–1.000). This step resulted in a reduction of the isotropic residuals (from $R(F)/R_w = 0.131/0.146$ to 0.096/0.107, respectively, for 30 variables and 2400 observed, unaveraged reflections) along with a general 4-fold reduction in the standard deviations of the positional and thermal parameters for all atoms. The final anisotropic refinement of all atoms (61 variables, 799 reflections) yielded $R(F)/R_w = 0.044/0.044$, with the largest residual peak of 1.72 e/Å³ at 1.07 Å from I1.

The Guinier powder pattern calculated with the refined structural model agreed very well with that observed for the bulk product with Si as an internal standard. This allowed indexing of the latter and a better determination of lattice constants, which were then used for distance calculations. Some data collection and refinement parameters are given in Table 1. The final atomic coordinates (origin at I), isotropic equivalent temperature factors, and their estimated standard deviations are listed in Table 2. Additional data collection and refinement information and the anisotropic displacement parameters are available as Supporting Information. The latter plus the structure factor data are also available from J.D.C.

Physical Property Measurements. Magnetic susceptibilities of β -K₄La₆I₁₄Os were measured on a 20 mg sample of the 90% synthesis

Table 1. Crystallographic Data for β -K₄La₆I₁₄Os^a

fw	2956.69
space group; Z	$P4/ncc$ (No. 130); 4
lattice constants (Å)	
a	13.117(3)
c	25.7(1)
V (Å ³)	4330(2)
d_{calc} (g/cm ³)	4.534
μ (Mo K α), (cm ⁻¹)	190.02
R, R_w ^b	0.044, 0.044

^a Cell constants were refined from Guinier powder pattern data with Si as an internal standard; $\lambda = 1.540 562$ Å; 22 °C. ^b $R = \sum ||F_o| - |F_c|| / \sum |F_o|$; $R_w = [\sum w(|F_o| - |F_c|)^2 / \sum w(F_o)^2]^{1/2}$; $w = \sigma_F^{-2}$.

Table 2. Positional and Isotropic Equivalent Displacement Parameters (Å²) for β -K₄La₆I₁₄Os^a

atom	Wykoff			x	y	z	B_{eq} ^b
	posn	site	sym				
Os	4c	4		0.25	0.25	0.1839(1)	1.01(4)
La1	4c	4		0.25	0.25	0.0669(1)	1.85(7)
La2	16g	1		0.1230(1)	0.0773(2)	0.18275(8)	2.06(7)
La3	4c	4		0.25	0.25	0.2993(1)	1.51(7)
I1	16g	1		0.3003(2)	-0.0904(2)	0.1779(1)	3.3(1)
I2	16g	1		0.1299(2)	0.0371(2)	0.3142(1)	3.1(1)
I3	16g	1		0.0990(2)	0.0558(2)	0.05445(8)	3.8(1)
I4	4c	4		0.25	0.25	0.4330(2)	4.5(1)
I5	4b	4		-0.25	0.25	0	5.3(2)
K	16g	1		0.4554(9)	-0.192(1)	0.0745(4)	6.4(6)

^a Origin at $\bar{1}$. ^b $B_{\text{eq}} = (8\pi^2/3) \sum_i \sum_j U_{ij} a_i^* a_j^* a_i a_j$.

product (above) that was loaded in a He-filled glovebox into an improved fused-silica container.¹⁸ The magnetic susceptibilities were measured at 3 T over the range 6–300 K on a Quantum Design MPMS SQUID magnetometer. The magnetization of the sample was first checked as a function of the applied field between 0 and 6 T at 50 and 100 K to screen for possible ferromagnetic impurities, but these were found to be insignificant ($M(T) \rightarrow 0$ at $H = 0$). The data were corrected for the susceptibility of the container and for the standard diamagnetic core contributions.

Calculations. EHMO calculations were carried out on the isolated cluster La₆(Os)I₁₈⁸⁻ with all bonded iodines and the observed dimensions using the suite of programs developed by R. Hoffmann and co-workers at Cornell University. The atom parameters were the same as cited elsewhere.¹²

Results and Discussion

Synthesis. The apparent increase in variety among reduced rare-earth-metal cluster halides has at the same time increased synthetic problems, since multiple products have been found in, for example, the ternary Y–I–Ru¹⁹ and Pr–I–Ru^{20,21} systems. In the K–La–I–Os system, the phases recognized so far include KLa₆I₁₀Os (isostructural with KPr₆I₁₀Os⁸), K₂La₆I₁₂Os,¹¹ and the two types of K₄La₆I₁₄Os.¹² Experiments carried out to prepare the previously known tetragonal α -K₄La₆I₁₄Os¹² from the ideal composition instead yielded the present β -K₄La₆I₁₄Os. The isoelectronic and isostructural Fe and Ru versions of the latter are stable as K₄Pr₆I₁₄Fe and K₄Pr₆I₁₄Ru, but not with lanthanum. Exploratory reactions with an Rb₄La₆I₁₄Os composition resulted instead in yet another structure.²² The α -polytype was usually obtained from somewhat more reduced

(18) Guloy, A. M.; Corbett, J. D. *Inorg. Chem.* **1996**, *35*, 4669.

(19) Payne, M. W.; Ebihara, M.; Corbett, J. D. *Angew. Chem., Int. Ed. Engl.* **1991**, *30*, 856.

(20) Payne, M. W.; Dorhout, P. K.; Corbett, J. D. *Inorg. Chem.* **1991**, *30*, 1467, 3112.

(21) Payne, M. W.; Dorhout, P. K.; Kim, S.-J.; Hughbanks, T.; Corbett, J. D. *Inorg. Chem.* **1992**, *31*, 1389.

(22) Uma, S.; Corbett, J. D. Unpublished research.

(14) Payne, M. W.; Corbett, J. D. *Inorg. Chem.* **1990**, *29*, 2246.

(15) Sheldrick, G. M. *SHELXS-86*; Universitat Göttingen: Göttingen, Germany, 1986.

(16) TEXSAN, Version 6.0; Molecular Structure Corp.: The Woodlands, TX, 1990.

(17) Walker, N.; Stuart, D. *Acta Crystallogr.* **1983**, *A39*, 159.

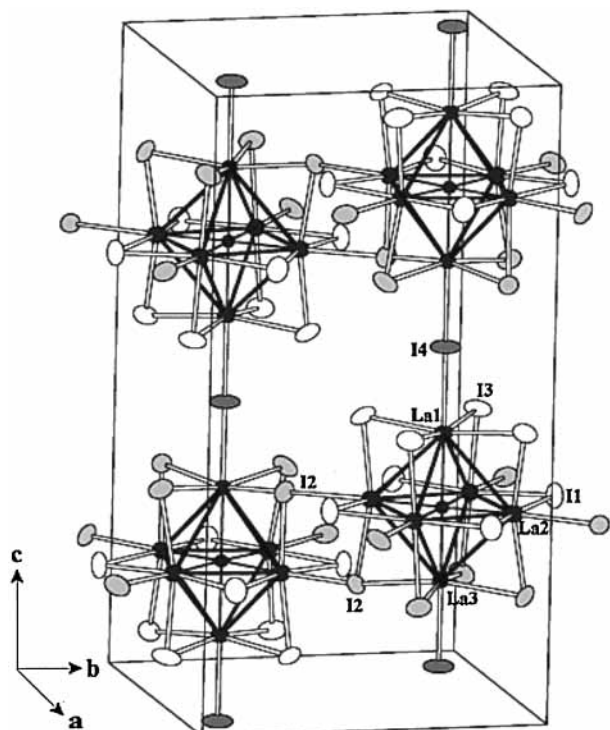


Figure 1. \sim [100] view of the La₆(Os)I₁₃ anionic cluster network in the unit cell of β -K₄La₆I₁₄Os, together with the atom-numbering scheme (90% probability ellipsoids). I^I ellipsoids are white, I^a and I^{-a} are gray, and La and Os are black. K₄I³⁺ ions lie in alternate columns of the cell at $c = 0, 1/2$.

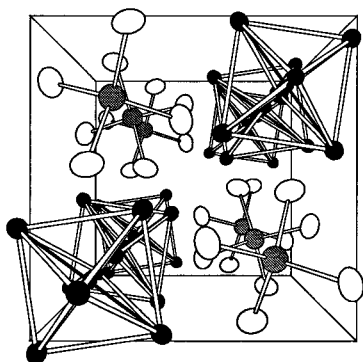


Figure 2. \sim [001] view of the columns of K₄I³⁺ cations and La₆Os clusters in the anion chains in β -K₄La₆I₁₄Os. All iodine atoms on the latter have been omitted for clarity.

compositions, but this distinction is weakened by the fact that the initial loading is always oxidized somewhat by the formation of some LaOI from adventitious H₂O. Both phases were obtained in one preparation. There is probably a small compositional difference between the two phases rather than a temperature-dependent feature, but the level is not apparent from X-ray structural refinements.

Structure. β -K₄La₆I₁₄Os crystallizes in the space group $P4/ncc$ with a new structure type in which a network composition R₆X₁₃Z³⁻ is filled with well-separated (K₄I)³⁺ units. The general theme of the former is noncentrosymmetric clusters trans-bridged by I^{4^{-a}} atoms into cluster strings that lie on the 4-fold axes along $1/4, 1/4, z$ and $3/4, 3/4, \bar{z}$, Figure 1. These are interrelated by $\bar{1}$ symmetry at $1/2, 1/2, 1/2$ and a 222 point at $1/2, 1/2, 1/4$, etc. The K₄I³⁺ units lie at 4 positions $1/4, 3/4, 0; 3/4, 1/4, 0$; etc. Figure 2 shows the arrangement of isolated metal clusters (without bound I) and the (K₄I)³⁺ units as viewed along [001]. The central feature is an La₆ cluster formed by three crystallographically

Table 3. Important Interatomic Distances (Å) and Angles (deg) in K₄La₆I₁₄Os

Os–La1		2.944(4)	I3–La1	3.242(3)
Os–La2	×4	2.812(2)	I3–La2	3.257(3)
Os–La3		2.905(4)	I3–K	3.70(1)
			I3–K	3.85(1)
La1–La2	×4	4.051(4)	I4–La1	3.370(6)
La2–La2	×2	3.977(3)	I4–La3	3.366(5)
La3–La2	×4	4.063(3)	I4–K	×4 3.94(1)
			I5–K	×4 3.37(1)
La1–I3 ⁱ	×4	3.242(3)	K–I1	3.56(1)
La1–I4 ^{a-a}		3.370(6)	K–I2	3.80(1)
La2–I1 ⁱ		3.202(3)	K–I3	3.85(1)
La2–I1 ⁱ		3.230(3)	K–I3	3.71(1)
La2–I2 ^{i-a}		3.353(3)	K–I4	3.94(1)
La2–I2 ^{a-i}		3.435(3)	K–I5	3.37(1)
La2–I3 ⁱ		3.257(3)		
La3–I2 ^{i-a}	×4	3.229(2)	I3–La1–I3	168.9(1)
La3–I4 ^{a-a}		3.366(5)	I1–La2–I1	165.76(9)
			I2–La2–I3	165.43(9)
I1–La2		3.203(3)	I2–La3–I2	166.6(1)
I1–La2		3.230(3)	La2–I2–La3	156.53(9)
I1–K		3.56(1)		
I2–La2		3.353(3)		
I2–La2		3.435(3)	K–I5–K	×2 112.4(3)
I2–La3		3.229(2)	K–I5–K	×2 108.0(2)
I2–K		3.80(1)		

distinct metal atoms and centered by an Os atom at $1/4, 1/4, 0.184$, etc. (Figure 1). The Os and the apical La1 and La3 atoms lie on the 4-fold axes along c , while the La2 atoms constitute the equatorial plane of a nominal octahedral unit. The symmetry of the cluster is in fact reduced to C_4 by the unusual iodine bridging mode, which is reflected by the spread among the La–Os distances ($\Delta = 0.132(4)$ Å, Table 3). The octahedra are unsymmetrically elongated along the La1–Os–La3 axis so that the apical La1–Os and La3–Os distances are about 0.14 and 0.09 Å greater than the 4-fold equatorial La2–Os distance. Similarly, the difference among three different La–La separations is 0.186(4) Å.

The 12 edges of the rare-earth-metal cluster are bridged by three crystallographically different iodine atoms to form the well-known La₆I₁₂ unit, but in an unusual manner (Figure 1). Each cluster has four I1 and four I3 atoms with the functionality I^I that bridge the four La2–La2 edges around the cluster waist and four La1–La2 edges at one end, respectively. Four more I2 atoms bridge the remaining La2–La3 edges, but these induce an asymmetry in the cluster as they are also I^{-a} in character and form exo bonds to La2 atoms in the four other clusters lying in diagonal directions normal to c (Figure 2). Each bridge is, as usual, opposed by another I2 atom on the other cluster that links to apices on the central cluster as I^{a-i}. The symmetry is such that these I2 intercluster bridges occur alternatively on the top and bottom halves of the clusters, which generates chains that are alternately displaced “up and down” along \bar{c} (Figure 1). The longer range effect is corrugated layers, a portion of which are shown in Figure 3. Finally, two I4 atoms link the different layers via I^{a-a} linear bridges at the apical La1 and La3 of each octahedron. The different La–Iⁱ distances are similar and average 3.237 Å, while I2^{-a} is 0.124 Å closer to the La3 apex, where it participates in the intercluster bridging, than to La2 at the cluster waist. As usual, the bonds with functions La–I^{a-i} and La–I^{a-a} are longer, 3.37–3.44 Å. The shortest I^I–I contact, 4.158 Å, is between I1 atoms in two clusters in the same layer (Figure 1), not a particularly close encounter.

The present La₆I₁₃Os network creates just the right cavity for the K₄I³⁺ unit (or vice versa) (Figure 4). The isolated I5 occurs on a $\bar{4}$ site and is four-bonded only to K. The latter is

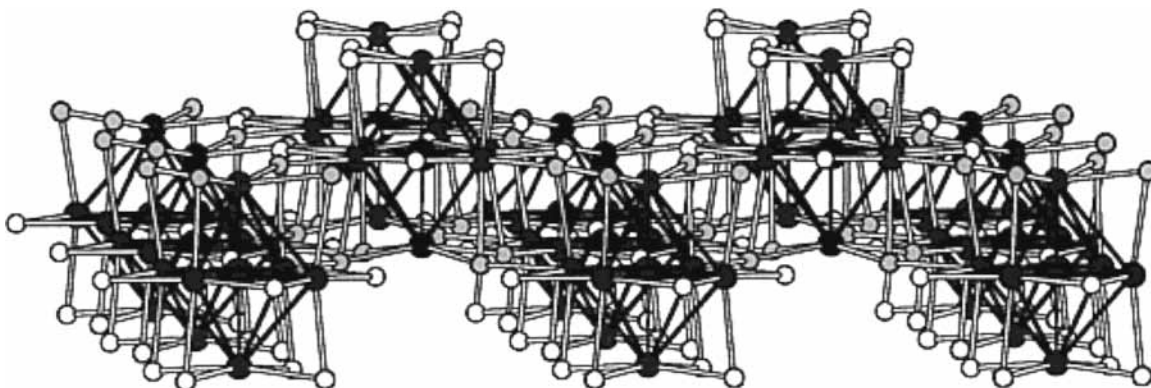


Figure 3. Portion of a corrugated layer of interbridged clusters in β - $\text{K}_4\text{La}_6\text{I}_{14}\text{Os}$.

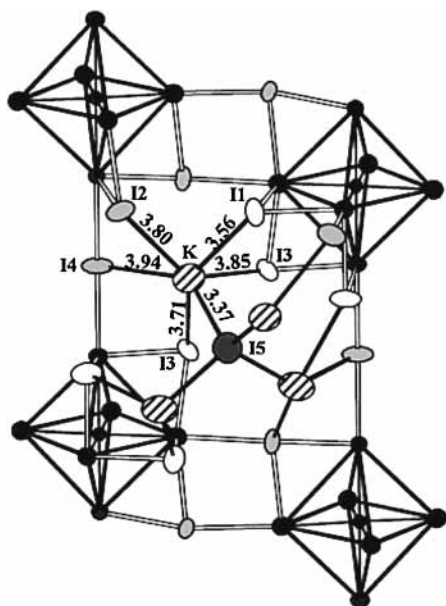


Figure 4. Environment about K (striped) and the lone I5 (dark gray) in β - $\text{K}_4\text{La}_6\text{I}_{14}\text{Os}$. The bridging I ellipsoids are light gray, and inner I, open (90%).

six-coordinate to the unique I5, one I^{2i-a} , two I^3 , one I^1 , and one I^{4a-a} over a rather large distance range, the last five falling between 3.56 and 3.94 Å. The average K–I distance for all neighbors is 3.70 Å, a somewhat loose environment according to the crystal radius sum (3.58 Å) for I and K (CN6).²³ On the other hand, the bonding within K_4I^{3+} is clearly tight, $d(\text{I5} - \text{K}) = 3.37 \text{ \AA} \times 4$, 0.20 Å less than the crystal radius sum (CN4), so that the identification of this as a distinctive unit is reasonable. Even larger differences from crystal radii were found within K_4Br^{3+} and $\text{Cs}_4\text{Br}^{3+}$ cations (0.27, 0.51 Å) in the somewhat halogen-rich zirconium cluster bromides $(\text{K}_4\text{Br})^{3+}(\text{Zr}_6\text{Br}_{18}\text{B})^{3-}$ and $(\text{Cs}_4\text{Br})^{3+}(\text{Zr}_6\text{Br}_{16}\text{B})^{3-}$.¹³ Certainly the presence of K_4I^{3+} critically depends on the “fit” of this cation into the network. Analogous compounds could not be obtained from individual substitutions of Rb, Fe, or Ru in the lanthanum compound, while the other two group 8 transition metals did work as (K_4I) - $(\text{Pr}_6\text{I}_{13}\text{Z})$, Z = Fe, Ru.

The interconnection pattern for the anion network in $(\text{K}_4\text{I})^{3+}(\text{La}_6\text{I}_{13}\text{Os})^{3-}$ can be written $\text{La}_6(\text{Os})\text{I}_8\text{I}^{i-a}{}_{4/2}\text{I}^{a-i}{}_{4/2}\text{I}^{a-a}{}_{2/2}$. This is general for R_6X_{13} stoichiometries, but different spatial relationships among the four I^{i-a} bridged edges give different structures. For example, in the monoclinic $\text{Cs}_4\text{R}_6\text{I}_{13}\text{Z}$ (R = Ce, Pr; Z = Co, Os),⁷ the bridging to other clusters occurs through

two cis edges plus a second trans pair related by inversion at Z to give layers of tilted clusters that are again connected at trans vertexes by I^{a-a} . In the present case, the halogen bridging in the layer leaves adjoining clusters staggered but parallel (Figure 3). For the tetragonal ($I4_1/amd$) $\text{Cs}_4\text{Pr}_6\text{I}_{13}\text{C}_2$ and $\text{Cs}_4\text{Sc}_6\text{I}_{13}\text{C}_4$,⁴ the I^{i-a} atoms above opposed edges in one half of the octahedron are related to the other two by a 4_1 axis along the chain, so that a three-dimensional network is produced. Zirconium examples of orthorhombic $\text{Zr}_6\text{Cl}_{13}\text{B}$ and $\text{KZr}_6\text{Cl}_{13}\text{Be}$ and the related tetragonal $\text{Zr}_6\text{Cl}_{11.5}\text{I}_{1.5}\text{B}^{24}$ exhibit the unusual Cl^{i-i} and Cl^{a-a-a} functionalities and very different structures. The presence of tetrahedral $(\text{K}_4\text{I})^{3+}$ ions distinguishes the present R_6X_{14} composition from the many $\text{Zr}_6\text{X}_{14}(\text{Z})$ and $\text{Nb}_6\text{Cl}_{14}$ ²⁵ compounds with a unique three-dimensional network $(\text{Zr}_6\text{Z})\text{X}_{10}\text{X}^{i-a}{}_{2/2}\text{X}^{a-i}{}_{2/2}\text{X}^{a-a}{}_{4/2}$. The only other M_6X_{14} -type structure so far is the polymorph α - $\text{K}_4\text{La}_6\text{I}_{14}\text{Os}$ with a layered interconnection pattern $(\text{La}_6\text{Os})\text{I}_8\text{I}^{i-a}{}_{4/2}\text{I}^{a-i}{}_{4/2}\text{I}^{a-a}{}_{2/2}$ for D_{4h} clusters that generate a unique planar network of clusters parallel to the a - b plane.

Properties. The transition-metal interstitial contributes both electrons and orbitals for the formation of strong bonds within the octahedral rare-earth-metal clusters, and 18 cluster-based electrons are optimal for nominally octahedral R_6X_{12} -type clusters that are centered by transition elements. This corresponds to the R–Z bonding MO's a_{1g}^2 and t_{2g}^6 , the R–R bonding HOMO t_{1u}^6 , and the nominally nonbonding e_g^4 on Z.³ The 16-electron cluster in β - $\text{K}_4\text{La}_6\text{I}_{14}\text{Os}$ shows an average elongation of 0.112 Å in $d(\text{La} - \text{Os})$ along the La1–Os–La3 axis relative to the four equatorial bonds (Table 3) along with asymmetric bridging about La3. All other clear distortions observed for 16-electron “octahedral” clusters have involved tetragonal compressions.^{11,14,26} Magnetic susceptibility measurements on β - $\text{K}_4\text{La}_6\text{I}_{14}\text{Os}$ (Figure 5) reveal only a temperature-independent (van Vleck-like) paramagnetism, $\sim 4 \times 10^{-4} \text{ emu} \cdot \text{mol}^{-1}$ after core corrections, which implies a closed-shell configuration. (The χ_0 value is comparable to those found for several other rare-earth-metal and zirconium cluster halides.^{11,27}) This must result from splitting of the octahedral t_{1u}^4 into an e_u^4 HOMO. EHMO calculations on the cluster unit $\text{La}_6(\text{Os})\text{I}_8$ with the observed proportions do indeed show a splitting in this direction, but only by 0.07 eV when all iodines are given the same input parameters. The calculated split should be enhanced by the use of a higher H_{pp} value for the bridging I^{2i-a} and I^{2a-i} .

(24) Köckerling, M.; Qi, R.-Y.; Corbett, J. D. *Inorg. Chem.* **1996**, *35*, 1437.

(25) Simon, A.; von Schnering, H.-G.; Wöhrle, H.; Schäfer, H. *Z. Anorg. Allg. Chem.* **1965**, *339*, 155.

(26) Hughbanks, T.; Corbett, J. D. *Inorg. Chem.* **1989**, *28*, 631.

(27) Steinwand, S. J.; Corbett, J. D. *Inorg. Chem.* **1996**, *35*, 7056.

(23) Shannon, R. D. *Acta Crystallogr.* **1976**, *A32*, 751.

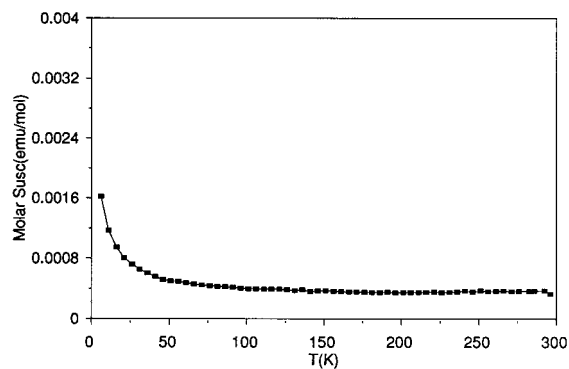


Figure 5. χ_M ($\text{emu}\cdot\text{mol}^{-1}$) for β -K₄La₆I₁₄Os as a function of T (K) at 3 T.

The synthesis of β -K₄La₆I₁₄Os once again emphasizes the possibility of new structures that can be produced by subtle variations in such quaternary systems, e.g., even the atom sizes.

The presence of the new K₄I³⁺ ion in this reduced rare-earth-metal cluster compound suggests the possibility of other new structures with different R:X ratios that may be created with the aid of suitable counteranions and minor alterations in the sizes of the components. Alkaline-earth-metal substituents are virtually unexplored.

Acknowledgment. We thank Jerome Ostenson for the magnetic data. This research was supported by the National Science Foundation, Solid State Chemistry, via Grant DMR-9510278 and was carried out in the facilities of Ames Laboratory—DOE.

Supporting Information Available: Tables of additional data collection and refinement parameters together with anisotropic displacement parameters for β -K₄La₆I₁₄Os. This material is available free of charge via the Internet at <http://pubs.acs.org>.

IC990072V